Ceramics International 42 (2016) 11958–11965

Contents lists available at ScienceDirect

Ceramics International

journal homepage: www.elsevier.com/locate/ceramint

Rare earth metals' influence on the heat generating capability of cobalt ferrite nanoparticles

Constantin Virlan [a], Georgiana Bulai [b], Ovidiu Florin Caltun [b], Rolf Hempelmann [c], Aurel Pui [a,*]

[a] Faculty of Chemistry, "Alexandru Ioan Cuza" University of Iasi, Carol I Bd., no. 11, 700506 Iasi, Romania
[b] Faculty of Physics, "Alexandru Ioan Cuza" University of Iasi, Carol I Bd., no. 11, 700506 Iasi, Romania
[c] Saarland University, Physical Chemistry, 66123 Saarbrüken, Germany

ARTICLE INFO

Article history:
Received 24 March 2016
Received in revised form
21 April 2016
Accepted 21 April 2016
Available online 22 April 2016

Keywords:
Rare earth
Doped cobalt ferrite
Nanoparticles
Hyperthermia
XRD
EDX
SAR analysis

ABSTRACT

The aim of this study is to synthesize and assess the potential applications of rare earth doped cobalt ferrite nanoparticles in cancer treatment through hyperthermia.

The synthesis of $CoFe_{2-x}RE_xO_4$ (where RE=Yb, Dy, Gd and x=0.01–0.3) through the co-precipitation method is presented. The composition and properties of the nanoparticles where investigated and evaluated in correlation with their heat generating capability. The XRD and EDX analysis indicated phase separation for high rare earth content with the appearance of Gd_2O_3 and Dy_2O_3 secondary phases, which leads to unwanted changes in the nanoparticles' magnetic properties and consequently of the specific absorption rate. All the nanoparticles present functional group belonging to the surfactant as determined by FT-IR and Raman. Magnetic and specific adsorption rate measurement suggest increases in saturation magnetization and SAR value in doped ferrites, compared to $CoFe_2O_4$ with as much as 26% and 15% for Dy doped and Gd doped samples respectively.

1. Introduction

In recent years the interest towards the applications of pristine and doped cobalt ferrites has increased due to their specific properties, which allows for their use in various fields such as catalysis [1], and photocatalysis [2], as gas sensors [3], actuators [4], as well as in medicine. The medical applications for ferrite nanoparticles, cobalt ferrite in particular, include contrast agents [5], hyperthermia treatment [6,7], controlled drug delivery [8] as well as combinations of these three applications.

A large number of synthesis method have been developed to obtain simple and mixed ferrites for various applications such as hydrothermal [9], sol-gel [10], co-precipitation methods [11,12], of which the latter is the most used, allowing for a good control over composition, size and morphology, as well as low costs and high efficiency.

In order to obtain nanoparticles for applications in hyperthermia, specific magnetic properties must be obtained. To the best our knowledge, this is the first study that gives results on the specific absorption rate of a series of cobalt ferrite nanoparticles doped with different rare earth cations. An increasing interest is given to nanoparticles with high saturation and remanent magnetization and large coercive field. These properties could lead to an increase in the specific adsorption rate of the nanoparticles, therefore improved efficiency in raising the temperature inside the targeted medium [6].

2. Materials and methods

2.1. Synthesis of nanoparticles

Cobalt ferrite nanoparticles doped with rare earth metals with general formula $CoFe_{2-x}RE_xO_4$ (where RE=Yb, Dy, Gd and x=0.01; 0.03; 0.05; 0.1; 0.2; 0.3) were synthesized through the co-precipitation method with carboxymethyl cellulose as natural surfactant, a variation of the method described in previous works [13].

The synthesis was performed through co-precipitation in basic media using NaOH to control the pH, at 80–90° C for one hour followed by repeated washing in order to remove NaCl and calcination at 500 °C for 6 h in air.

2.2. Structural and morphological characterization

The structural characterization of the samples was performed using powder X-ray diffraction by an X-ray diffractometer (LabX XRD-6000) with CuKα radiation (λ=0.15406 nm). FT-IR analysis was done using a Fourier transmission infrared spectrometer

* Corresponding author.
E-mail address: aurel@uaic.ro (A. Pui).

http://dx.doi.org/10.1016/j.ceramint.2016.04.121
0272-8842/

(Jasco 660 Plus) in KBr disks, in the 4000–400 cm^{-1} range and in CsI disks in the 600–250 cm^{-1} range with a resolution of 4 cm^{-1}. The Raman spectra were recorded using a Renishaw inVia Reflex confocal microscope equipped with a He–Ne laser at 633 nm (17 mW) and a CCD detector coupled to a Leica DM 2500 M microscope in the 100–900 cm^{-1} range. The major hysteresis loops were recorded using a Model 3900 Vibrating Sample Magnetometer System (VSM) at room temperature. The morphology of the samples was evaluated using transmission electron microscopy coupled with energy dispersive X-ray spectroscopy (EDX) using a JEOL JEM-2010 Electron Microscope.

2.3. Evaluation of specific adsorption rate

The specific adsorption rate was measured using the calorimetric method in alternating radiofrequency field with a frequency of 400 kHz using a Huettinger Elektronik Type 20 generator with a maximum power of 4.5 kW. The colloidal solution was placed in a double walled vessel connected to a Lauda RE 104 thermostat set at 25 °C. The temperature was measured using an optical thermo sensor Optocon Fotemp 1 with a resolution of 0.1 °C. The SAR values were calculated using Eq. (1) [14,15].

$$SAR = \frac{C}{x} \cdot \frac{dT}{dt} \quad (1)$$

where C is the specific heat of the medium (4.185 J/g for water), x is the fraction of the ferrite and dT/dt is the initial slope of the temperature versus time curve.

3. Results and discussions

3.1. Material characterization

The **XRD** patterns for the calcined samples indicate the formation of pure phases for most of the compounds even at high dopant concentration. The formation of secondary phases is visible for Dy and Gd doped ferrites starting with $CoFe_{1.8}Dy_{0.2}O_4$ and $CoFe_{1.7}Gd_{0.3}O_4$ respectively, and is represented by the rare earth oxides as presented in Fig. 1. In the case of Yb doped cobalt ferrite the obtained nanoparticles are of the highest purity with perfectly indexed pattern and no visible unassigned peaks. For the Gd doped particles a secondary Gd_2O_3 phase was identified for the highest dopant concentration ($CoFe_{1.7}Gd_{0.3}O_4$) most likely due to the larger ionic volume of gadolinium. The dysprosium cobalt ferrites present the most evident phase separation although its ionic volume is almost as large as that of Gd and can be attributed to its thermal properties, as Dy has the highest melting point amongst the three rare earths used in the study.

The above mentioned phase separations have been previously described in other works for similar systems and synthesis methods as well as different methods (i.e. ceramic), and were ascribed to the large atomic volume difference between iron or cobalt and rare earth metals such as dysprosium and gadolinium for which the phase separations were more visible [16–18].

The crystallite size of the nanoparticles was determined using by averaging the values obtained by applying Scherer's equation on the six most intense peaks. The results indicate that the particles have crystallite sizes ranging between 15 and 25 nm and do not vary significantly especially for the Dy and Gd doped ferrites. The crystallite size can be correlated with electron microscopy images and has a great influence on the magnetic properties and specific adsorption rate of the nanoparticles. The calculated values for the average crystallite size as calculated are summarized in Table 1.

The XRD and FT-IR data also offer important information regarding the cation redistribution in the crystal lattice supported by the displacement of the XRD peaks (thus changes in the lattice parameter) and in the FT-IR spectra in the 600–250 cm^{-1} region, specific for metal-oxygen bonds.

Taking into account the considerably larger cation volume for the rare earth metals compared to iron and cobalt it would be expected to see an increase in the lattice parameter as it would significantly distort the tetrahedral and octahedral lattices. This behavior is especially visible for Gd doped ferrites with small amounts of rare earth and barely visible for Yb doped ferrites,

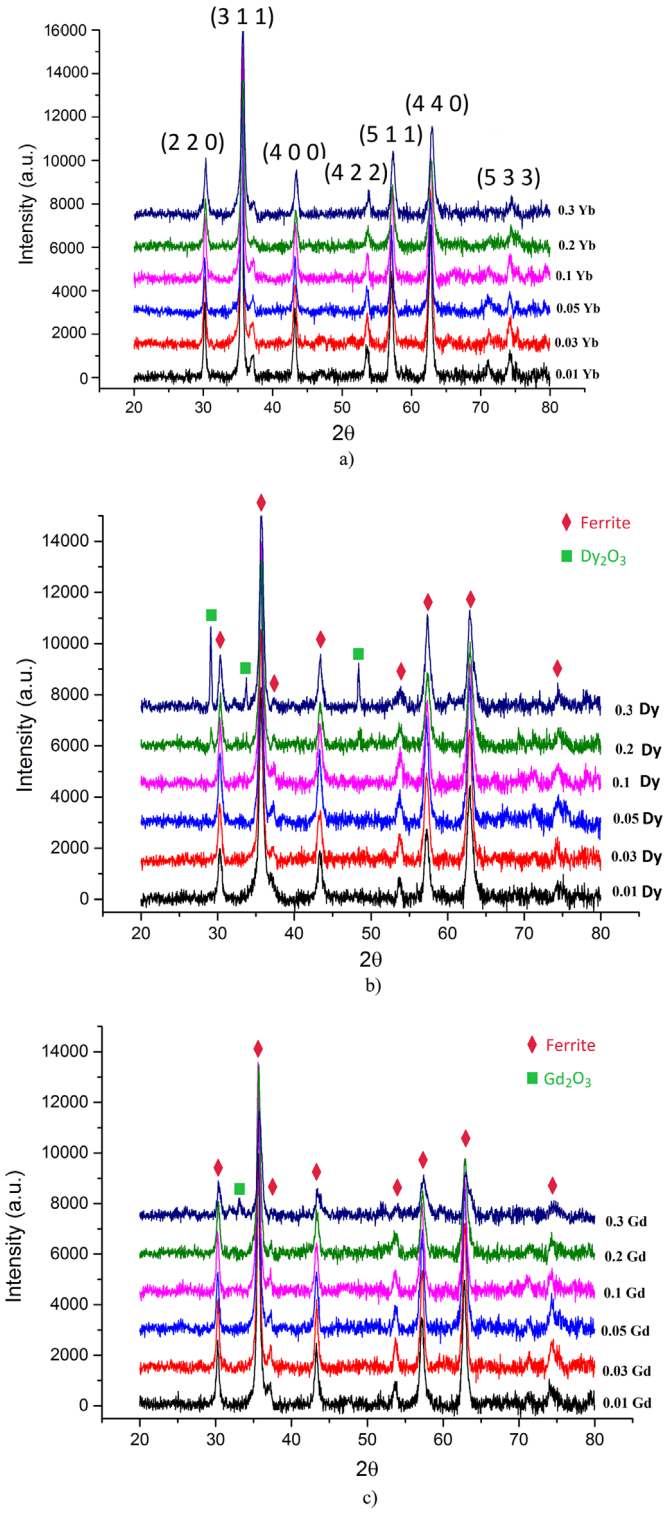

Fig. 1. XRD patterns of $CoFe_{2-x}RE_xO_4$, where RE=Yb (a); Dy, (b) and Gd, (c).